International Journal of Engineering Research & Technology (IJERT)
ISSN: 2278-0181
Vol. 4 Issue 05, May-2015

Effect of Desulfovibrio Desulfuricans on Zn and $Zn_{17}Al_3$ Alloy Fabricated Ductile Iron

Suman Dutta[1]
Research Scholar, Dept. of Chemistry,
Jadavpur University,
Kolkata-700032, W.B., India

Pritish Majumdar[3]
Emeritus Scientist, Dept. of Metallurgical Eng. and
Material Science, Jadavpur University,
Kolkata-700032, W.B., India

Swapan Kumar Bhattacharya[2*]
Professor, Dept. of Chemistry,
Jadavpur University,
Kolkata-700032, W.B., India

Bidhan Chandra Ray[4]
Retired Professor, Dept. of Chemistry,
Jadavpur University,
Kolkata-700032, W.B., India

***Abstract* - Microbial influenced corrosion of Zn (422 gm/m2) and Zn17Al3 alloy (436 gm/m2) coated ductile iron were investigated in presence of sulphate reducing bacteria desulfovibrio desulfuricans (DD) in aqueous solution using mass loss and electrochemical measurements. The specimens were exposed in DD medium for different number of days ranging from 2 to 80 to investigate the change in corrosion rates with time. The results suggest that the open circuit potential shifts to more negative values with increased exposure time and high corrosion current is obtained in presence of bacteria in comparison to abiotic medium for both samples. Electrochemical and mass loss results demonstrate that DD accelerated pitting propagation damage due to increase in both cathodic and anodic reaction rates. Presence of DD leads to formation of a dense and thick layer of oxide and hydroxide of zinc and iron, suggest propagation of the corrosion attack beneath the oxide layer.**

Keywords: Zn, $Zn_{17}Al_3$ alloy coating; Microbial corrosion; desulfovibrio desulfuricans; Pitting corrosion; Potentiodynamic polarization.

I. INTRODUCTION

Corrosion has been recognized as one of the most dominant forms of the detoriation process and identified as the major cause of the loss of coating from pipelines. Corrosion may attack the pipelines either internally, or externally, or both. External corrosion is a major factor contributing to the detoriation of buried pipelines by weakening the pipe wall, which increases the risk of failure. Even though buried pipelines are protected with coatings and cathodic protection, the pipelines are still vulnerable to various types of corrosion mechanisms. There are many types of bacteria that can lead to corrosion initiation or increase the corrosion rate such as sulphate reducing bacteria (SRB), acid producing bacteria, iron oxidizing bacteria, nitrate reducing bacteria etc. Among them SRB is regarded as one of the most troublesome groups of bacteria influencing the microbial influenced corrosion (MIC). The mechanism of action of SRB is usually attributed to the chemical corrosiveness of H_2S, facilitated H^+ reduction at deposited FeS and biological consumption of chemically formed H_2. MIC is one of the possible threats to buried pipelines because corrosive bacteria grow well in muddy soil environment. Reviews of bacterial corrosion were published by Postgate [1] and Booth [2]. Booth and his colleagues had made impressive progress in establishing that cathodic depolarization is a major mechanism of anaerobic corrosion by SRB, correlating corrosion rates and polarization curves [3] with the hydrogenase contents of the strain and species used. Anodic processes may influence the corrosion rate in certain strains, however. The biological corrosion of coated ductile iron has received increasing consideration in the last few decades [4-12].

Zn and Zn-Al coated ductile iron have been used increasingly for pipes for supply of drinking water, drainage, cooling towers system etc. due to its corrosion resistance, mechanical workability and resistance to bio-fouling [3]. But Zn and $Zn_{17}Al_3$ alloy coatings are susceptible to localized damage in presence of corrosive electrolytes and different corrosive bacteria. Zn and $Zn_{17}Al_3$ alloy coatings protect iron against corrosion by the two following effects: a barrier effect due to the continuity of the coating that separates the iron from the corrosive environment and a galvanic protection because zinc and aluminium act as a sacrificial anode to protect the underlying iron [1, 2]. Usually, a thickness of 55 µm (defined by European standard NBN EN 10240 as 396 g/m^2) is advised for good protection of steel against generalized corrosion in fresh water. However, a coating in which the zeta phase is absent or too thick and presents a columnar morphology [13-16], does not protect iron from generalized corrosion. To be efficient, the outer η-layer must represent at least 45% of the thickness of the whole coating [13].

Extrapolation of Tafel lines is one of the most popular DC techniques for estimation of corrosion rate. The lines for charge transfer controlled reactions give the corrosion current density, i_{corr} at the corrosion potential, E_{corr}. Two thumbs rules should be applied when using Tafel extrapolation. For an accurate extrapolation, at least one of the branches of the polarization curve should exhibit linear of the semi logarithmic scale over at one decade of current density. In addition, the extrapolation should start at least 50-100 mV away from E_{corr}. These two rules improve the accuracy of manual extrapolations [17]

With respect to the determination of corrosion rate, the most accurate and precise method is probably that of mass loss. This is because the experimentation is easy to replicate and, although long exposure times may be involved, the relatively

simple procedure reduces the propensity to introduce systematic errors [18-20]. Electrochemical measurements depend on many parameters that can affect the obtained results. Whereas electrochemical measurements may be the most rapid, they are also the most susceptible to variations in conditions [17].

Till now only few studies described bio-corrosion of galvanized pipelines by SRB. A. Seth et al. [21] have noticed frequent occurrences of SRB in drinking water when cast iron pipes are used. They indicated SRB's ability to colonize a new installation quickly, causing an increase of corrosion rate. Ilhan-Sungur et al. [10] observed a corrosion rate of galvanized steel was 3 µm/y in abiotic environment. The rate in corresponding biotic environment was 12 µm/y. Moreover, they showed that galvanized steel could be corroded by microorganisms as well as SRB. They assessed that SRB could survive in the mixed species bio-film with very high Zn concentrations. Likewise, a study outlines an increase of corrosion rate from 6 µm/y in abiotic environment to 9.5 µm/y in biotic environment for carbon steel [22]. In some cases, the corrosion rate of galvanized steel can reach 20 µm/y if conditions are favourable to bacterial growth [23].

Due to metabolic activities of microorganisms, structure of inorganic passive layer on metal surface changes and increase their dissolution and removal from metal surface. However more researches are needed to investigate corrosion caused by SRB in aqueous environments, since the marine environments have a high SRB concentration. The aim of present study is to gain better understanding of corrosion characteristics and electrochemical behavior of Zn and $Zn_{17}Al_3$ alloy coated ductile iron in DD environment using open circuit potential, electrochemical measurement, scanning electron microscope (SEM), and mass loss techniques.

II. EXPERIMENTAL MATERIALS AND METHODS

2.1 Microbial culture:

The bacteria used in this study were desulfovibrio desulfuricans (NCIM No. 2047). A new culture was resuscitated from freeze dried ampoule and was subcultures twice in 5 ml of modified media. After resuscitation, the bacteria were cultured for 3 days in a 250 mL Erlenmeyer flask containing 50 ml of the fresh culture medium on a rotary shaker (33ºC, 150 rpm). A total of 50 mL of the cultured bacteria, stored in a 4ºC refrigerator, was used as the inoculums in all of the experiments to ensure a monoculture of the desulfovibrio desulfuricans bacteria. All the flasks were capped with stoppers to prevent contamination by airborne bacteria. To maintain the bacterial density at the steady-state growth phase throughout the study period a semi continuous mode of SRB culture growth was employed, that is, 75% of the medium every 7 days was drained and replaced with an equal amount of a fresh sterile medium. All the experiments were carried out in a batch process at 33ºC in an incubator. In order to maintain the uniformity the chloride level and oxygen level the temperature is kept constant for the all solutions.

2.2 Microbiological Cultivation and inoculation.

DD was cultivated separately in appropriate media and grown in modified Postgate's 'C' medium after a thorough deoxygenated step by passing nitrogen gas. Postgate's 'C' [1] medium for desulfovibrio desulfuricans consists of 0.5gm/L K_2HPO_4, 1.0gm/L NH_4Cl, 2.0 gm/L Na_2SO_4, 2.0 gm $MgSO_4$ $7H_2O$/L, 0.004 gm/L $FeSO_4$, 0.006 gm/L $CaCl_2$ $6H_2O$, 1.0 gm/L yeast extract, 0.39gm /L $C_6H_5CO_7Na_3$, 10 ml 60% sodium lactate as an electron donor and carbon source per litre water. The solutions were autoclaved at 121°C for 20 min at 1 barr pressure then stored at room temperature until use. The pH was then adjusted to 7.4 through addition of 0.1M KOH. The solution was then poured into the test cell after proper dilution with sterilized water with bacterial solution. All the experiments were made at ambient temperature.

2.3 Preparation of specimens:

Square shaped specimens with dimension 1 cm^2 were used for electrochemical measurements, rectangular shaped specimens with dimensions 3×2 cm^2 were used for bio-film observation and immersion test. Prior to the experiments, each specimen was sequentially rinsed with sterile water thrice, degreased in acetone, followed by sterilizing in 70% ethanol and dried aseptically in a laminar flow cabinet. The newly prepared specimens were immediately immersed in the test medium for all of the corrosion experiments or kept in desiccators until used.

2.4 Electrochemical cell and equipment

A standard three-electrode ASTM electrochemical cell was utilized in all electrochemical experiments. The reference electrode was saturated calomel electrode (SCE) separated from the cell by a glass frit. The counter electrode was a Pt-foil (1cm^2). Polarization curves were determined potentiodynamically with a scan rate 0.5mV/s. The working electrode was coated ductile iron with Zn and $Zn_{17}Al_3$ alloy and sealed with epoxy resin to give two-dimensional surface (1cm^2) exposed to the electrolyte with bacteria. All the surface-area dependent values reported in this paper (current, resistance) are normalized with respect to geometric surface area of the electrode. The electrochemical measurements were performed using Sycopol-AEW-3(1000 mA/1amp) potentiostat (Sycopol Scientific Electrochemistry Software). The experiments were conducted in a 150 ml volume cell at room temperature. Polarization measurements were carried out starting from cathodic potentials of -2 volt to an anodic potential of +2 volt with respect to corrosion potential.

2.5 Mass loss measurement:

Mass–loss measurements were carried out at room temperature according to the ASTM standard G1-72 [24].These coupons were kept immersed in biotic SRB for 1200 hrs along with a control set (abiotic) medium. The difference between the final and initial was reported as mass loss. Before and after each experiment, the coupons were dried and weighed using an analytical balance (precision ±0.1mg) and the mean mass loss is reported in the paper.

C.R $= \frac{K \times W}{A \times t \times d}$ mg $dm^{-2}day^{-1}$; Where K = 2.40×10^6, t = time of exposure (h), A = Area of coupon (cm^2), w = mass loss after cleaning (mg), d = density of the corroding metal (mg cm^{-3}).

2.6 Surface analysis:

The coated test coupons were observed for surface bio-film and corrosion features using SEM. The coupons with bio-film were immersed for 15min in 4% glutaraldehyde solution in order to fix the bio-film on the coated sample surface, and then become dehydrated using four ethanol solutions (15 min each): 25%, 50%, and 75% successively. After that, the samples were taken to the SEM for their surface analysis. We have seen that bacteria cells attached and formed a bio-film layer on the Zn and $Zn_{17}Al_3$ alloy coated surfaces.

II. RESULTS AND DISCUSSION

3.1 Mass loss measurement:

The results of the mass loss study showed that desulfovibrio desulfuricans caused increase in mass loss compared to sterile medium. The difference in corrosion rates in sterile abiotic and SRB media was significant. Variations in mass loss and corresponding corrosion rate observed for coated ductile iron were shown in Fig. 1. Mass loss of the specimens increased during the first 92 hrs of Zn and 134 hrs for $Zn_{17}Al_3$ alloy on exposure in media containing SRB and reached a plateau after these periods. The maximum value of the mass loss determined was 0.6777 mg/cm^2 for Zn and 0.5237 mg/cm^2 for $Zn_{17}Al_3$ alloy in SRB medium after exposures of 450 hrs. The corrosion rate was seen to decrease with time from 3 to 1200 hrs. Over the past decades progress has been made to understand the interaction between the SRB activities within biofilm and the corrosion process of zinc coating. The typical reactions of MIC due to SRB can be expressed as:

Anodic reactions: $Zn \rightarrow Zn^{2+} + 2e^-$ (1)

$2Al \rightarrow 2Al^{3+} + 6e^-$ (2)

Electrolytic dissociation of water:

$8H_2O \rightarrow 8H^+ + 8OH^-$ (3)

Cathodic reaction: $8H^+ + 8e^- \rightarrow 8H$ (4)

Cathodic depolarization by SRB:

$SO_4^{2-} + 8H \rightarrow S^{2-} + 4H_2O$ (5)

Corrosion product: $Zn^{2+} + S^{2-} \rightarrow ZnS$ (6)

Corrosion products: $Zn^{2+} + 2OH^- \rightarrow Zn(OH)_2$ (7)

$Zn(OH)_2 \rightarrow ZnO + H_2O$ (8)

Another Corrosion products: $2Al^{3+} + 3S^{2-} \rightarrow Al_2S_3$ (9)

$2Al^{3+} + 6OH^- \rightarrow 2Al(OH)_3$ (10)

$2Al(OH)_3 \rightarrow Al_2O_3 + 3H_2O$ (11)

Due to formation of above corrosion products in presence and absence of SRB, coatings of Zn and $Zn_{17}Al_3$ alloy dissolved and showed variation of corrosion rate.

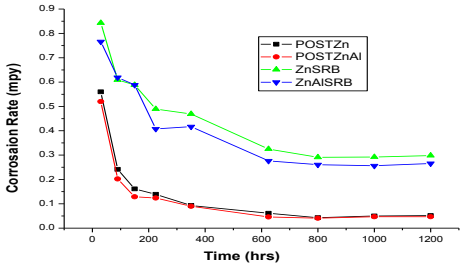

Fig. 1: Variation of corrosion rate of Zn and $Zn_{17}Al_3$ alloy in SRB culture solutions over exposure time/hr.

3.2 Open circuit potential (E_{ocp}):

Fig. 2 shows open circuit potential (E_{ocp}) over time for Zn and $Zn_{17}Al_3$ alloy coated ductile iron (DI) specimen immersed into the Postgate's 'C'media. It is seen from the curves of Zn and $Zn_{17}Al_3$ alloy in SRB culture that E_{ocp} shifts negatively first then shifts positively with time but shifting rate becomes smaller. It was seen from SEM picture the formation of oxidation film in the culture medium. The oxidation brittle products gradually form on the electrode surface during immersion. As can be seen E_{ocp} of Zn and $Zn_{17}Al_3$ alloy coated in sterile medium was relatively stable and reduced in the range between -0.1030V to -0.1067V and -0.1020V to -0.1056V (saturated calomel electrode, SCE) respectively throughout the 800 hrs of exposure. In SRB augmentation E_{ocp} of Zn and $Zn_{17}Al_3$ alloy coated ductile Fe decreased from -0.1034V to -0.1132 V and -1.017V to -1.102 V (SCE). The more decrease of E_{ocp} in presence of SRB is attributed either to weakening of Zn and $Zn_{17}Al_3$ alloy passivity of surface activation or to decrease in the cathodic process rate, for example due to decrease in the concentration of dissolved oxygen in tested medium. Marked decrease of E_{ocp} was detected after 40 h of Zn and 62 h of $Zn_{17}Al_3$ alloy coated coupons following the SRB augmentation. During further exposure thick sedimentation occurred specially in presence of SRB seemingly before formation of metal oxide and this tendency persisted. Due to increased sedimentation on metal surface, E_{ocp} of all specimens increased with time. This is due to the increased brittleness in surface texture developed with time for both pure Zn and $Zn_{17}Al_3$ alloy.

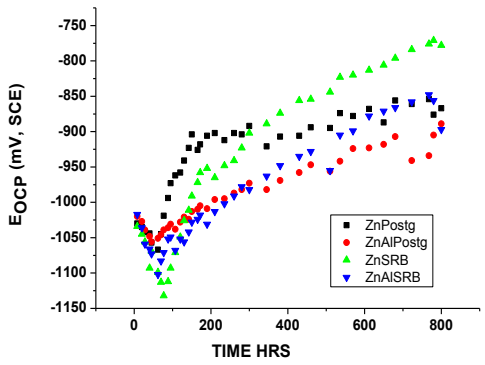

Fig. 2: Variation of open circuit potential (E_{ocp}) over time for thermal spray coated specimens of Zn and $Zn_{17}Al_3$ alloy in Postgate's 'C' media and with DD bacteria.

3.3 Tafel Polarization curves:

Polarization measurements, widely used [4, 10, 18, 23, 24] for monitoring instantaneous corrosion rates of a metal or alloy coating exposed to corrosion environment, are suitable for detection of changes of corrosion rate due to presence of bacteria and other corrosive species. Representative Tafel polarization curves have been recorded for Zn and $Zn_{17}Al_3$ alloy coated specimens in aqueous solutions in presence and absence of bacteria cultures solution at 30ºC. Due to non linear anodic slope, it is impossible to draw anodic Tafel slope only by Tafel extrapolation method [25]. Figures 3(a) - 6(b) show the potentiodynamic polarization curves of Zn and $Zn_{17}Al_3$ alloy coated ductile iron respectively in sterile nutrient Postgate's 'C' medium and SRB culture medium at

30ºC. The corrosion current densities, i_{corr} of Zn and $Zn_{17}Al_3$ alloy coated specimens remain relatively constant throughout the exposure time in Postgate's 'C' medium. During exposure of 17 days in Postgate's 'C' medium Zn coated specimens the corrosion current i_{corr}, slowly increases from 1.326 mA to1.823 mA . After 35 days i_{corr} decreases, then with exposure time extending beyond 40 days, i_{corr} increases and attains the high value of 1.880 mA after 80 days exposure. The corrosion current of $Zn_{17}Al_3$ alloy coated specimens also increase from 0.758 mA to1.430 mA after 17 days exposure then changes from 1.560 mA to 1.648 mA after 35 to 80 days of exposure in sterile nutrient Postgate's 'C' medium. The corrosion potential of Zn coated specimens, E_{corr}, undergoes a negative shift 52 mV (-1088 mV to -1140 mV vs SCE) with exposure time of 80 days and for $Zn_{17}Al_3$ alloy coated specimens, E_{corr} , undergoes a positive shift 46 mV (-1166 mV to -1112mV vs SCE) with exposure time of 80 days. These indicate of slight change of corrosion rate of the Zn and $Zn_{17}Al_3$ alloy coated specimens in Postgate's 'C' medium. This is probably attributable to the effect of chloride, sulphate, phosphate and lactate ions of the Postgate's 'C' medium on the passivation film on the anodic oxidation reaction. This phenomenon is consistent with the presence of a stable passivating Zn and Al rich oxide or hydroxide film on the coated surface. The formation of passivation films depends on the pH of the solution, chloride and sulphate ion concentration in the solution and composition of substrate on which they are formed. From the extrapolation of Tafel slope, Tafel constant β_a and β_c were computed and showed in table 1 and 3 for both specimens in Postgate's 'C' medium. The cathodic Tafel slope, β_a and β_c, show no discernible trends. They fluctuate in the range of about 308.0 mV. decade^{-1} to 377.8 mV. decade^{-1} for Zn coated specimens and 419.3 mV. decade^{-1} to 350.9 mV.decade^{-1} for $Zn_{17}Al_3$ alloy coated specimens**,** indicating that the cathodic oxygen reduction reaction is independent of exposure time. The anodic Tafel slope, β_a, remains more than 200 mV. decade^{-1} for both specimens in Postgate's 'C' medium throughout the exposure time, indicating that the anodic oxidation reaction is under diffusion control.

In presence of SRB in Postgate's 'C' the corrosion phenomenon Zn and $Zn_{17}Al_3$ alloy coated specimens are quite different as seen in table 2 and 4 and Fig 4(a), 6(a) respectively. During the exposure of 2 to 17 days , in SRB culture corrosion current , i_{corr} of Zn coated specimens increases slowly from 1.508 mA to 1.937 mA then for long term exposure of 35 days to 80 days exposure corrosion current increases from 2.142 mA to 3.989 mA and $Zn_{17}Al_3$ alloy coated specimens corrosion current , i_{corr} increase slowly during the exposure of 2 to 17 days from 1.275 mA to 1.738 mA and then for long time exposure of 35 to 80 days i_{corr} increase from 2.040 mA to 2.966 mA . These phenomena are attributed to the breakdown of the passivation film after the prolonged synergistic attack of SRB and aggressive chloride and sulphate anions and enzymes extracted from SRB. The corrosion potential, E_{corr}, undergoes a negative shift in the SRB -inoculated medium at the first stage of immersion. Up to 17 days E_{corr} shifts from -1114 mV to -1149 mV, and then shifts towards positive direction to -1088 mV after 80 days immersion Zn coated specimens in SRB culture and $Zn_{17}Al_3$ alloy coated specimens up to 17 days E_{corr} shifts from -1106 mV to -1175 mV after 12 days then shifts towards positive direction to -1114 mV after 65 days immersion. The phenomenon is caused by the colonization of SRB bacteria on the corroded metal surface and the subsequent modification of the chemical composition of the passive film on the coated surface. From the extrapolation of Tafel slope, Tafel constant β_a and β_c are computed and shown in table 2 and 4 for both specimens in SRB containing Postgate's 'C' medium. The value of anodic and cathodic Tafel slope β_a and β_c are quite irregular pattern and difficult to predict corrosion tendency from these data. For Zn coated specimens it is seen that after the exposure of specimens 2, 7, 50 and 65 days β_a decreases as compared to without SRB culture medium and for $Zn_{17}Al_3$ alloy coated specimens β_a decreases after 2 days immersion in SRB medium as compared to without SRB medium. These data indicate enhancement of the kinetics of anodic oxidation reactions under the attack of desulfovibrio desulfuricans bacteria. On the other hand, the relatively larger value of β_c, as compared to those specimens in sterile bacteria free medium, indicates that cathodic oxygen reduction reactions might be correlated with the development of bio-film of desulfovibrio desulfuricans. The above results reveal that Zn and $Zn_{17}Al_3$ alloy coated ductile iron specimens undergo different corrosion processes in the absence and presence of the desulfovibrio desulfuricans in Postgate's 'C' medium.

There is a tendency for polarization curves to shift to right i.e. to the higher current density of the Tafel plot in sterile to SRB solutions respectively. Tafel slope also indicates that the anodic polarization current density increases significantly and that the width of the passive range of potentials and corrosion potentials decrease in sterile to DD solutions in turn, indicating the corrosion current density is the highest in SRB and lowest in sterile abiotic medium. The width of the passive region in sterile medium is largest for Zn and $Zn_{17}Al_3$ alloy coated specimens [Fig. 3(a), 5(a)]. It was found that there was wide passive region for Zn and wider passive region for $Zn_{17}Al_3$ alloy in the presence of only SRB corresponding to without SRB culture medium.

It was seen that Zn and $Zn_{17}Al_3$ alloy coated specimens exposed in the culture medium was followed by formation of a dense and thick ZnO, $Zn(OH)_2$, ZnS , Al_2S_3 , Al_2O_3 etc layer over the corroded surface. It seems reasonable to suggest that propagation of the corrosion attack in SRB medium occurred beneath this oxide layer.

Also visible current increased on anodic curves due to oxide layer disruption by accumulation of corrosion products. Consequently, the anodic current increase occurred when the activated area beneath the oxide layer was finally exposed to the culture medium due to mechanical breakdown of the protective layer. In the present experiment the breakdown was observed at positive potential sweep usually associated with pit initiation.

However, the activated surface area by surface reducing bacteria DD has largely a statistical character strongly depending on the number of initiated pits, their deepness , diameter distribution over specimen surface, etc. , that may significantly vary from specimen to specimen. It is fair to expect that a large part of the biologically activated surface

[Fig. 7 and 8] will be accessible to the solution resulting in a sharp and beneficial increase in anodic current.

After the bio-film and corrosion products were removed from the surface of the coupons were re-examined by SEM, depletion of Zn in some regions of the test specimens were noted. Pitting corrosion of the coating was also observed (Fig. 9 and 10). However we didn't observe any pitting or depletion of zinc in abiotic medium.

The values of the corrosion rates presented in table 1-4 reveal that the rate increases with time for the two specimens in presence and absence of bacteria. The corrosion rates of Zn coated material are always greater than that of $Zn_{17}Al_3$ alloy both in presence and absence of microbes as expected. For both materials, the corrosion rate is significantly greater in presence of bacteria than that found in absence of it. To understand the role of bacteria in the mechanism of corrosion, the corrosion rate-time profiles are fitted with an equation of third order in power series, so that the equation becomes $R=A+Bt+Ct^2+Dt^3$. The values fitting parameters A-D in different system are presented in table 5. It reveals that R=A at t=0. Thus A represents the onset corrosion rate on exposing the samples in different media and the fresh metal surface at the beginning. As expected the initial corrosion as increases in the order: $Zn_{17}Al_3$ Postgate < $Zn_{17}Al_3$-SRB < Zn-Postgate < Zn-SRB. As the time passes pits and pores are generated on the surfaces. These increase the corrosion. Thus (B) values represent acceleration of corrosion due to generation of pits, pores and asymmetry on the surface. The acceleration (B) increases in the order Zn-SRB < $Zn_{17}Al_3$-SRB < Zn-Postgate < $Zn_{17}Al_3$ Postgate. In corrosive media corrosion acceleration is less than that of the corresponding Postgate medium because SRB accumulates at the surface causing blocking of pits and pores preventing further corrosion. The corrosion acceleration of $Zn_{17}Al_3$ alloy is greater than that of Zn because of more creation of pits and pores in the former due to mismatch of atoms(Zn and Al) inspite of their closeness in size and electro-positivity values. Third component of corrosion rate depends on the second power of time. It is mainly due to the accumulation of corrosion product which prevents ion conduction causing a negative component (decreasing trend in corrosion rate). The absolute value of the component varies in order: Zn-SRB < $Zn_{17}Al_3$-SRB < $Zn_{17}Al_3$-Postgate < Zn-Postgate. The fourth component of corrosion arises due to dissolution of base Fe for pore size-increment and complete removal of protective layer in some places. This +ve component follows the order: $Zn_{17}Al_3$-Postgate < Zn-Postgate < Zn-SRB < $Zn_{17}Al_3$-SRB. Here again this component is decreased in presence of SRB due to their accumulation on the base metal surface. The SRB may occupy the pits as residing places preventing opening of the bare metal, Fe.

Table 1 Analytical parameters of Tafel plot of Zn specimens in Postgate's 'C' medium after different exposure periods.

Exposure Time(days)	E_{corr} (mV)	i_{corr} (mA)	Corrosion Rate ($\mu m\ y^{-1}$)	β_a ($mV.decade^{-1}$)	β_c ($mV.decade^{-1}$)	E_{pp} (mV)	i_{pp} (mA)
2	-1088	1.326	3.083	207.8	308.0	-434.2	093.955
7	-1079	1.639	3.811	254.6	316.3	-347.0	083.660
12	-1080	1.796	4.176	172.4	340.3	-137.0	129.694
17	-1088	1.823	4.238	220.6	321.2	-477.8	088.088
35	-1096	1.703	3.959	169.2	334.3	-312.1	91.563
50	-1114	1.718	3.994	243.4	408.7	15.7	176.736
65	-1166	1.794	4.171	254.5	386.5	-233.7	116.982
80	-1140	1.880	4.371	220.1	377.8	-146.5	134.889

Table 2 Analytical parameters of Tafel plot of Zn specimens in SRB medium after different exposure periods.

Exposure Time(days)	E_{corr} (mV)	i_{corr} (m A)	Corrosion Rate(μ m y^{-1})	β_a ($mV.decade^{-1}$)	β_a ($mV.decade^{-1}$)	E_{pp} (mV)	i_{pp} (mA)
2	-1114	1.508	3.506	192.7	356.6	-172.6	131.377
7	-1122	1.767	4.108	262.1	402.5	-111.6	112.543
12	-1105	1.896	4.408	195.0	447.4	-85.4	121.596
17	-1149	1.937	4.504	211.7	476.0	-111.6	147.543
35	-1122	2.142	4.980	263.1	346.1	-68.0	120.038
50	-1061	2.418	5.622	180.8	431.6	277.2	109.678
65	-1058	3.272	7.607	265.9	508.4	-416.7	72.597
80	-1088	3.989	9.274	260.5	496.4	-503.9	82.588

Table 3 Analytical parameters of Tafel plot of $Zn_{17}Al_3$ alloy specimens in Postgate's 'C' medium after different exposure period.

Exposure Time(days)	E_{corr} (mV)	i_{corr} (m A)	Corrosion Rate(µm y^{-1})	β_a (mV.decade^{-1})	β_c (mV.decade^{-1})	E_{pp} (mV)	i_{pp} (mA)
2	-1166	0.758	1.762	196.4	419.3	-364.4	43.343
7	-1096	0.966	2.246	166	359.4	-59.3	128.032
12	-1105	1.366	3.176	177.6	313.6	-451.6	95.174
17	-1122	1.430	3.325	238.4	332.2	-329.6	81.530
35	-1115	1.560	3.627	176.8	302.5	-521.4	97.660
50	-1147	1.595	3.708	237.5	399.3	-146.5	131.377
65	-1131	1.622	3.771	240.1	388.2	1.700	159.412
80	-1112	1.648	3.832	235.3	350.9	-477.8	66.333

Table 4 Analytical parameters of Tafel plot of $Zn_{17}Al_3$ alloy specimens in SRB medium after different exposure times.

Exposure Time(days)	E_{corr} (mV)	i_{corr} (m A)	Corrosion Rate(µm y^{-1})	β_a (mV.decade^{-1})	β_c (mV.decade^{-1})	E_{pp} (mV)	i_{pp} (mA)
2	-1106	1.275	2.964	152.3	303.3	-469.0	095.174
7	-1114	1.426	3.315	192.9	319.4	-399.3	084.746
12	-1175	1.623	3.773	261.8	397.1	-190.8	112.543
17	-1140	1.738	4.041	264.1	336.1	-137.8	114.004
35	-1116	2.040	4.743	200.8	392.7	-155.2	155.353
50	-1140	2.291	5.327	257.9	386.9	-227.2	124.773
65	-1114	2.476	5.767	256.8	334.2	-469.0	88.088
80	-1131	2.966	6.896	257.6	353.5	-460.3	84.46

Table 5 The values of Polynomial fitting parameters A-D in different media of different specimens

Specimens	A	B	C	D
Zn-Postgate 'C'	+1.336	+0.043	-1.5×10^{-4}	$+8.73\times10^{-6}$
Zn-SRB	+1.543	+0.028	-5.064×10^{-4}	$+8.73\times10^{-6}$
$Zn_{17}Al_{13}$-Postgate 'C'	+0.6482	+0.065	-0.0013	$+8.8\times10^{-6}$
$Zn_{17}Al_{13}$-SRB	+1.175	+0.0443	-7.583×10^{-4}	$+6.03\times10^{-6}$

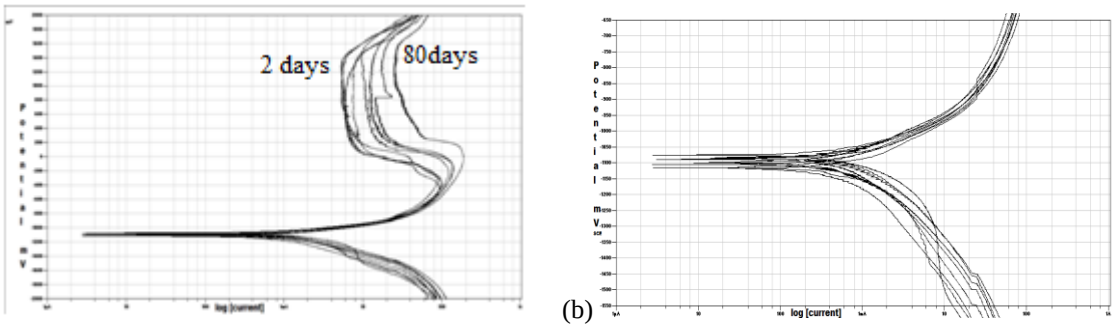

(a) (b)

Fig. 3(a) and 3(b) expanded: Tafel plots of Zn specimens in the sterile nutrient-rich medium after short-term exposure of 2, 7, 12 and 17 days, and long term exposure of 35, 50, 65 and 80 days.

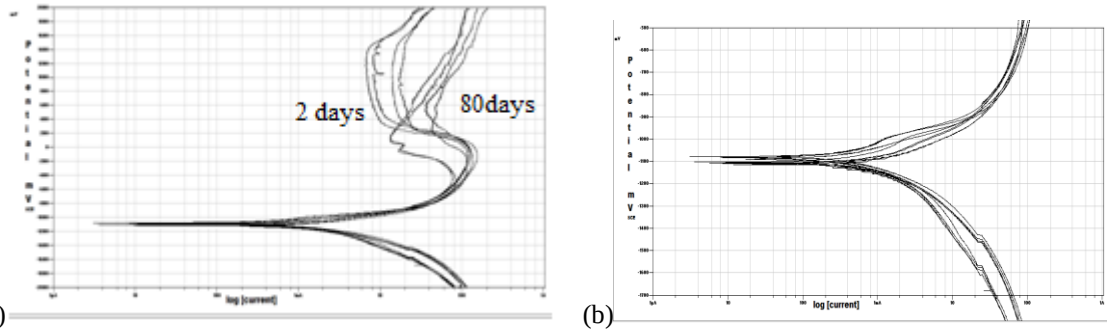

(a) (b)

Fig. 4(a) and 4(b) expanded: Tafel plots of Zn specimens in the SRB culture after short term exposure of 2, 7, 12 ,17 days and long term exposure of 35, 50, 65 and 80 days.

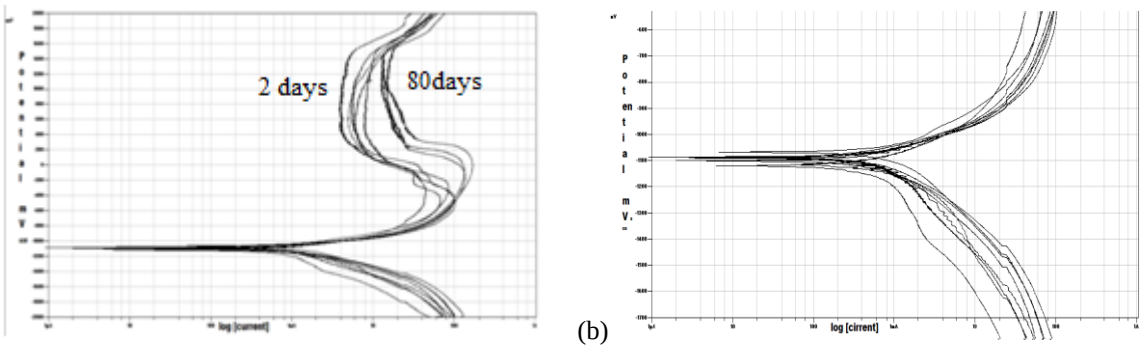

(a) (b)

Fig. 5(a) and 5(b) expanded: Tafel plots of $Zn_{17}Al_3$ alloy specimens in the nutrient-rich medium short term exposure of 2, 7, 12,17 days and long term exposure of 35, 50, 65 and 80 days.

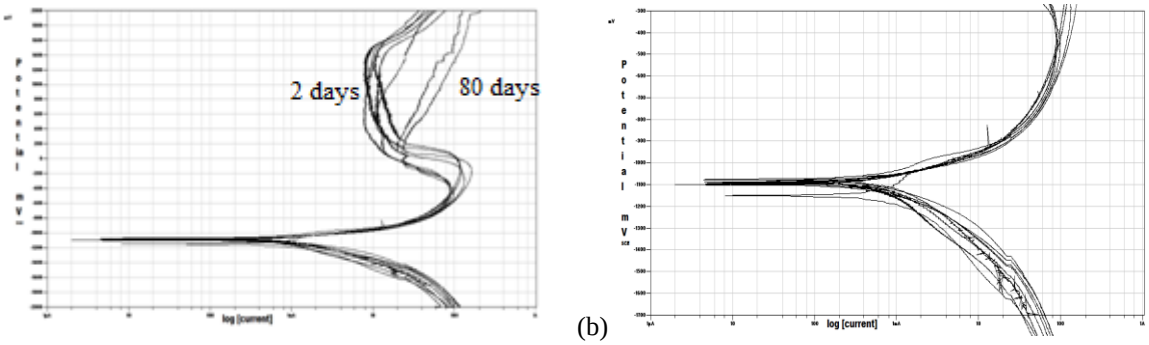

(a) (b)

Fig. 6(a) and 6(b) expanded: Tafel plots of $Zn_{17}Al_3$ alloy specimens in the nutrient-rich medium augmented with desulfovibrio desulfuricans after short term exposure of 2, 7, 12 and 17 days and long term exposure of 35, 50, 65 and 80 days.

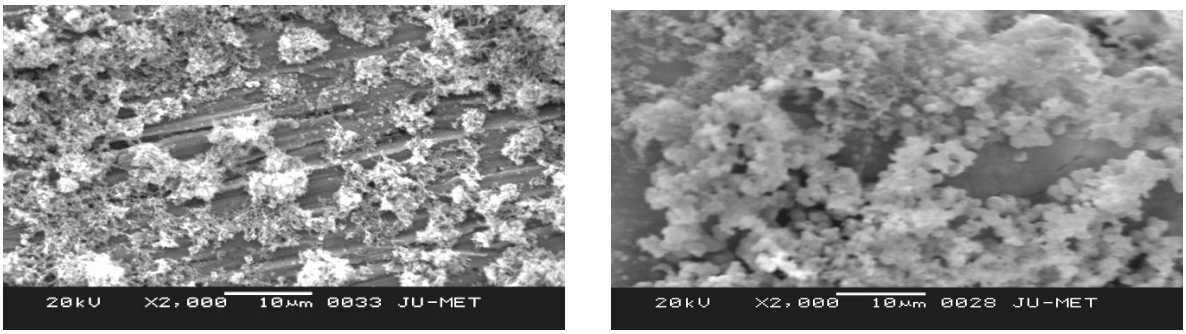

Fig. 7: SEM micrograph of desulfovibrio desulfuricans on Zn and $Zn_{17}Al_3$ alloy coated ductile iron specimen after 35 days immersion.

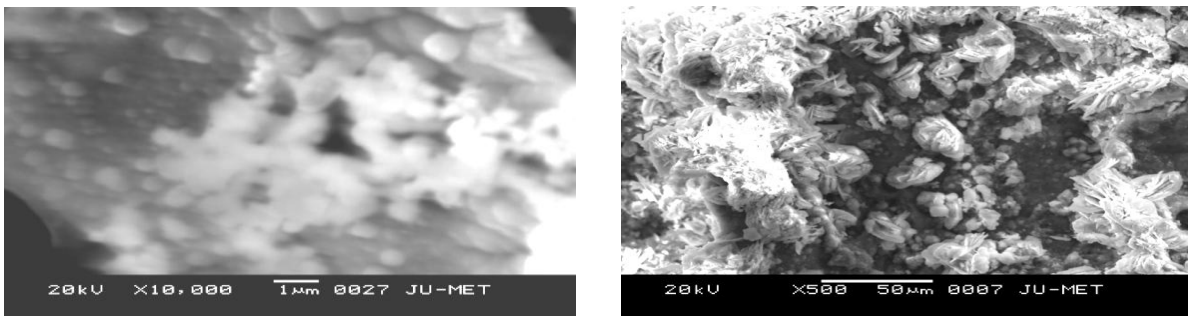

Fig. 8: SEM micrograph of desulfovibrio desulfuricans on Zn and $Zn_{17}Al_3$ alloy coated ductile iron specimen after 65 days immersion.

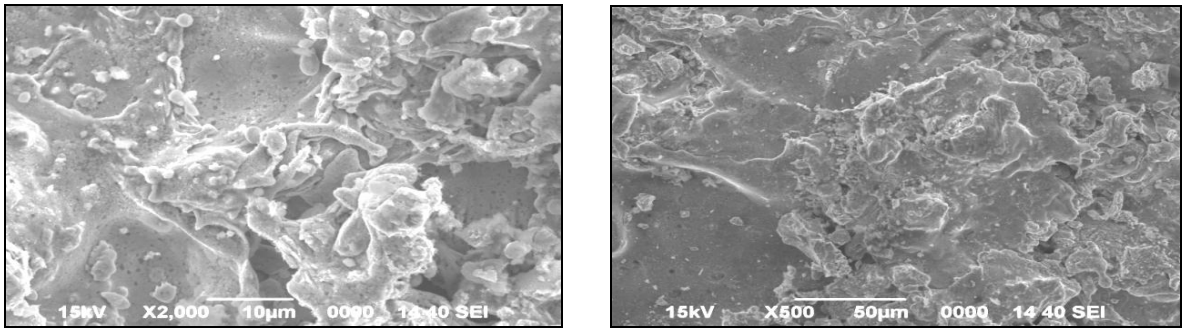

Fig. 9: SEM micrograph of Zn (422 gm/m^2) and $Zn_{17}Al_3$ alloy (436 gm/m^2) coated specimen after removal of corrosion products of 35 days.

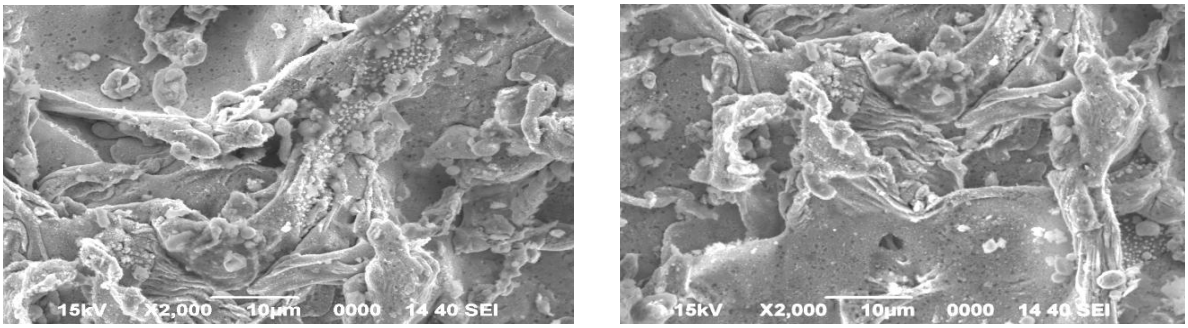

Fig. 10: SEM micrograph of Zn (422 gm/m^2) and $Zn_{17}Al_3$ alloy (436 gm/m$^{2)}$ coated specimen after removal of corrosion products of 65 days.

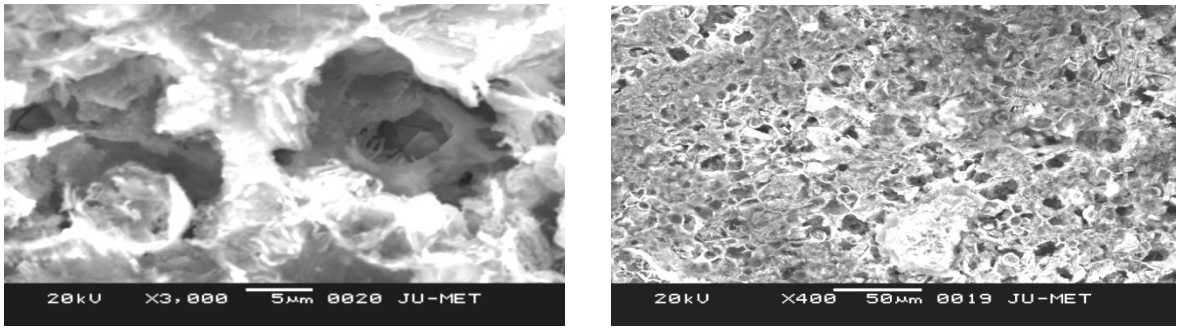

Fig. 11: SEM micrograph of Zn (422 gm/m^2) and $Zn_{17}Al_3$ alloy (436 gm/m^2) coated specimen after removal of corrosion products of 80 days.

3.7 Surface analysis

In order to characterize the various stages of corrosion propagation in SRB culture medium, surface morphology of Zn and $Zn_{17}Al_3$ alloy coated were examined at 20, 35, 65 and 80 days of exposure. As seen in Fig.7 and 8, there were rod and spherical shaped SRB cells in the coated surface, where a high cell density with a typical morphology of the genus (desulfovibrio) can be observed after 20 and 35 days immersion. At 12 days exposure specimens were covered with black FeS precipitate easily removed from the whole surface except small sites, which were covered with a dense deposit. On 20th day, the area of these sites significantly increased and after 35 days practically the whole surface was covered with a dense, brittle and lumpy deposit. Deposits covering the corroded surface sites had a layered structure. The upper layer of deposit contained spongy and needle shaped aggregates. Gravimetric analysis showed that these aggregates are oxide of zinc on Zn coated surface and these oxides along with Al_2O_3 and $Al(OH)_3$ on $Zn_{17}Al_3$ alloy coated surface. The pits eventually clearly seen on the surface where formed due to drying of specimen or mechanical removal of the upper layer (Fig 9, 10). After 50 days numerous annular damages showed up on the inner layer as sites of localized corrosion and become distributed over the whole surface indicating pitting corrosion attack. At this corrosion stage the majority of the pit mouths were covered with a round cap. Following exposure of 65 days the pit numbers increased significantly (Fig. 10). In addition to wide and deep pits, the inner oxide was fully perforated by numerous narrow pits (Fig. 11) after 80 days. In contrast, very small shallow pits were observed on the specimen exposed to the Postgate's 'C' medium without culture medium on Zn and $Zn_{17}Al_3$ alloy coated surface.

CONCLUSIONS:

1. Electrochemical analysis indicates that E_{corr} and i_{corr} in sterile medium remained virtually unchanged with exposure time, indicating that localized corrosion didn't occur on Zn and $Zn_{17}Al_3$ alloy coated surface of ductile iron and these coatings are relatively stable in sterile medium. SRB leads to distinct decrease in E_{corr} and increased i_{corr}, reveals surface activation by SRB and the chemicals produced by them.

SEM morphology has also shown that Zn and $Zn_{17}Al_3$ alloy coated surface suffers less oxide formation in sterile medium. However micrometer-scale pitting corrosion was observed on the metal surface in SRB solution.

2. The synergies between the metal surface, abiotic corrosion products and bacterial cells and their metabolic products influenced the pitting corrosion damage of the passive film and accelerated the pitting corrosion process.

3. Relatively low corrosion resistance of Zn coated specimens than $Zn_{17}Al_3$ alloy coated was detected when specimens are placed in SRB solution.

4. Strong decrease in corrosion resistance of Zn and $Zn_{17}Al_3$ alloy coated surface as a function of exposure time, was detected when specimens were placed at the bottom of the container and remained prolonged period of time into a layer of biogenic hydroxide sediments. Pitting corrosion attack was detected on the surface of "bottom" specimens. $Zn_{17}Al_3$ alloy coated specimens showed higher resistance to pitting corrosion in SRB medium.

6. SEM images of the surface and interface revealed that heterogeneity and coverage of biofilm formed on the specimens' surface increased with time and micro-pitting corrosion occurred under the biofilm.

7. In comparison, no apparent signs of pitting corrosion were observed on the specimens' surface upon short-term exposure in the Postgate's 'C', except the formation of thin conditioning layers. Even after a long term exposure only sparse and minor pitting corrosion had occurred on specimens of abiotic medium.

REFERECES:

[1] J. R. Postgate. The microbiology of corrosion, Corrosion handbook, vol. 1. 1963. p. 2.51-2.64.
[2] G. H. Booth. Sulphur bacteria in relation to corrosion. J. Appl. Bacterial vol. 27, 1964, p.174-181.
[3] W. Lee, Z. Lewandowski, P. H. Nielsen, et al., Bio-fouling, vol. 8, 1995, p.165-194.
[4] E. Ilhan-Sungur, A. Cotuk, vol. 104, 2005, p.211-219.
[5] I. B. Beech, C. W. Sunny Cheung, C. S. Patrick Chan, M. A. Hill, R. Franco. vol. 34, 1994, p.289–303.
[6] Duan, J. Z., Hou, B. R., Yu, Z. G, Mat. Sci. Eng. Vol. 26, 2006, p 624-629.
[7] H. A. Videla, L. K. Herrera, Int. Microbial. vol. 8, 2005, p. 169–180.
[8] F. A. Lopes, P. Morin, R. Oliveira, L. F. Melo, J. Appl.Microbial.,vol.101(5) ,2006, 1087-95.
[9] A. D. Seth and R. G. J. Edyvean, vol. 58, 2006, p. 108-111.
[10] E. Ilhan-Sungur, A. Çotuk, Corr. Sc., vol. 52 (1) 2010, p. 161-171.
[11] V. Barranco, S. Feliu., S. Feliu, Corr. Sc., 46 (9) ,2004, p. 2203-2220.
[12] R. Javaherdashti, Anti-Corr. Meth.Mater. , 46 (3), 1999, p. 173-180.
[13] A. R. Marder, Mat. Sci, 45 (3), 2000, p. 191-271.
[14] C. Volk, E. Dundore, J. Schiermann, M. Lechevallier, Water Res., vol. 34 (6), 2000 p.1967–1974.
[15] D. Quantin, M 1 530 2004, p. 1-7.
[16] Hot-Dip Galvanizing for Corrosion Protection: A Specifiers Guide, American Galvanizers Association, 2006, p.1-21.
[17] R. Kelly et al., 2002. P. 45.
[18] R. F. Sandenbergh, E. Van der Ling. Corros. Sci. 47, 2005, p. 3300–3311.
[19] A. I. Vogel, Textbook of Quantitative Inorganic Analysis, fourth ed., Longman, New York, 1978.
[20] P. J. F. Griffiths, J. D. R. Thomas, second ed., Edward Arnold, London, 1971.
[21] A. D. Seth and R. G. J. Edyvean, vol. 58 , 2006, p. 108-111.
[22] L. Carpen, P. Rajala, M. Vepsalainen, M. Bomberg, Euro. Corr. 2013, p. 1589.
[23] E. Ilhan-Sungur, N. Cansever, A. Cotuk, Corr. Sc., 49 (3) 2007, p.1097-1109.
[24] American Society for Testing and Material, G1-72, American Society for Testing Materials, Philadelphia, 1975, p. 626–629.
[25] J. Tafel, Z. Physik. Chem. Vol. 50 , 1905, p. 6661.